Progress In Electromagnetics Research C, Vol. 123, 197–212, 2022

A Foam-Based Compact Flexible Wideband Antenna for Healthcare Applications

Kailash V. Karad[1, 2, *] and Vaibhav S. Hendre[1]

Abstract—In recent times, the study of flexible wireless devices has attracted ample attention in the fields of biomedicine and healthcare. Biomedical systems are becoming more popular and employed to find harmful elements within human bodies. A portable biomedical device makes use of a contacting or non-contacting way to find tumours inside the human body. In view of this, a compact two-slot hexagonal shape flexible wideband microstrip antenna for healthcare application is presented. The proposed antenna is designed using a low-cost, light-weight, and broadly accessible flexible foam material. The slots incorporated into the geometry have enriched the percentage bandwidth of 106.67% with a total gain of 4.67 dBi. The flexible wideband antenna of dimension $28 \times 26 \times 2$ mm^3 is fabricated using copper foil. The designed and fabricated antenna operates over the frequency of 2.94 to 9.66 GHz resulting in three different resonating frequencies; 3.8 GHz, 6.7 GHz, and 9.1 GHz. The flexible antenna is tested under different bending conditions and obtains good performance to substantiate flexibility. The Specific Absorption Rate (SAR) analysis is also performed over a three-layer tissue equivalent body model and observes a maximum SAR value of 1.9 W/kg less than the safety limit of 2 W/kg for 10 gm of tissue. A good agreement is observed between the simulated and measured results of the proposed antenna for free space and human proximity.

1. INTRODUCTION

Wearable antennas are very much popular nowadays due to their compact size, shape, light weight, flexibility, and conformal nature. The world of electronics and communication attracts such antennas for various applications such as military, RADAR, healthcare, public safety, and many more. These antennas are more popular specifically in health monitoring systems because of their light-weight structure, low cost, and low maintenance. The 5G network is near adoption in several nations [1], as it offers significant improvements with less consumption of energy in wireless data rates, connectivity, bandwidth (BW), coverage, latency, and so on [2]. The Internet of Things (IoT) is a new technology [3] that aims to connect everything using many wireless device integrations and impact most of the traits of life and business in applications such as healthcare [4].

Wearable gadgets are supposed to be an indispensable part of the IoT, and it will increase the amount of traffic to 277 petabytes per month or even greater than that also as per the annual report [5] of Cisco of Virtual Networking Index (VNI, 2014–2019). Wearable utensils are utilized in the healthcare profession to monitor patients' vital health problems. A glucose monitoring device is used to monitor the patient's blood sugar level; a capsule endoscopy is used to check the patient's inner digestive system; and a wearable Doppler unit and thermometer are used to screen the patient's heartbeat, blood pressure, and body temperature respectively [6–8]. Researchers [9] have fabricated their antennas on flexible

Received 12 June 2022, Accepted 16 August 2022, Scheduled 2 September 2022

* Corresponding author: Kailash Vaijinath Karad (karadkv@gmail.com).

[1] Department of Electronics and Telecommunication Engineering, G. H. Raisoni College of Engineering and Management, Pune 412207, India. [2] GES's R. H. Sapat College of Engineering, MS & R, Nashik 422005, India.

materials to achieve flexibility and conformability. Nevertheless, textiles, polyimides, polyester film, and foam have all been tested and proven flexible [10, 11].

Generally, practical data transmission of these devices takes place with the help of on-body sensors and off-body routers. In on-body communication, sensors placed closely communicate with each other; however, the data from these sensors are sent to the remote off-body communication for analysis by the physician and doctor [12]. In today's technology world, wearable devices can be worn over different body parts like the arm, wrist, chest thigh, etc. and help to sense and monitor various body parameters such as temperature, pulse rate, humidity, sugar level, blood pressure, and calories burned [13].

Wireless body area networks (WBANs) have come a long way in recent years, demonstrating tremendous promise in a variety of healthcare applications. As illustrated in Figure 1, different wearable sensors provide the WBAN with additional capabilities, including electrocardiography (ECG), electroencephalography (EEG), temperature, sweat, motion, etc. Various physiological signals can be captured in this way and collected by the base station (BS) to aid in the delivery of preventative healthcare [14].

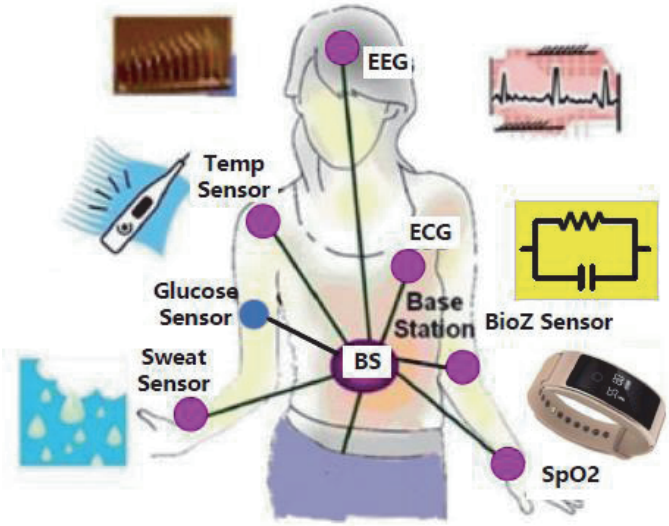

Figure 1. Body parameters measurement with different sensors [14].

Several publications have been recently published that discuss wearable antennas of various sizes, profiles and geometries including planar monopole antennas, microstrip patch antennas, Artificial Magnetic Conductor (AMC), Electromagnetic Band Gap (EBG) based monopole antennas, dual-polarized antenna for body-centric systems, dual-band dual-mode textile-based PDMS substrate antennas, etc. However, the main attention of all these wearable antennas is found in the ISM band or dual bands of frequency 2.4 GHz and/or 5.2–5.8 GHz. In addition to this, researchers have obtained wearable antennas for multiple-input multiple-output (MIMO) to get high data for biotelemetric devices. Also, to retain and optimize the bandwidth of wearable antennas, researchers have focused on the wideband type of wearable antennas which will be extensively useful for biomedical applications.

Even though all of the antennas described have good results, several of them suffer from their enormous size and narrow impedance bandwidth. Furthermore, a few antennae are made on expensive and scarce substrates. Although expensive substrates produce good outcomes, their scarcity forces the use of low-cost, readily available substrates over expensive ones. In [15], A dual-band triangular slotted monopole antenna is presented for WBAN applications operated at 3.5 GHz and 5.8 GHz for WiMAX wireless applications and ISM band respectively. An Artificial Magnetic Conductors (AMC) array [16] geometry is used to achieve high gain and low SAR. Rogers ULTRALAM 3850 substrate is used to print the antenna, and the AMC array is printed on substrate RO3003. The proposed antenna [17] is based on a conventional circular patch antenna configuration with PDMS as a substrate, and a full ground plane is maintained in the design. The PDMS substrate of relative permittivity 2.8 at 2.45 and

5.8 GHz, along with loss tangents of 0.02 and 0.04, is considered respectively.

A circularly polarized MIMO antenna for a wearable biotelemetric device is presented [18]. A square patch (SP) with modification in terms of a truncated corner is made to obtain circular polarization. An FR-4 substrate ($\varepsilon_r = 4.4$) with a thickness of 1.6 mm is used to print the antenna. It consists of four orthogonally placed antennas. This antenna covers the ISM band from 2.40 to 2.48 GHz and exhibits stable radiation, high gain, and high efficiency appropriate for high data wearable biotelemetric devices. In [19], the authors have presented a wideband low profile semi-flexible wearable antenna operative at a frequency of 2.4 GHz for biomedical telemetry applications. A rectangular patch with semi-flexible material of RT/duroid 5880 having $\varepsilon_r = 2.2$, $\tan\delta = 0.0004$ and partial ground is incorporated to increase the bandwidth of the structure. The overall dimension of 17 mm × 25 mm × 0.787 mm is used to design the geometry. The authors reported the negligible effect of antenna bending over the parameters like reflection coefficient, bandwidth, gain, and efficiency.

A wearable triangular patch antenna [20] for on-body WBAN is designed using a vinyl polymer-based flexible substrate to function in the ISM band with a centre frequency of 2.45 GHz. The designed prototype has compact dimensions $0.318\lambda_0 \times 0.318\lambda_0 \times 0.004\lambda_0$. To obtain high impedance bandwidth, a triangular patch is converted into Koch fractal geometry, and meandering slits with DGS have helped to get a maximum gain of 2.06 dB. A wearable dual-band antenna with a magnetoelectric dipole [21] is designed using a felt substrate of 3 mm thickness ($\varepsilon_r = 1.3$, $\tan\delta = 0.044$), for WBAN and WLAN applications. The wideband characteristic and low backward radiation are achieved by creating two slots of U shape in the dipole. The maximum gain reported is about 4.7 dB. The presence of a ground plane makes microstrip antennas the best applicant for body-worn devices. The low cost of fabrication, conformability, light weight, the comfort of on-body integration, and virtuous isolation between human body biological tissues and the antenna are the features of the microstrip antenna which make it the preeminent candidate [22].

The authors in [23] proposed an antenna on a flexible resin-coated paper of thickness 135 µm using a conductive nanoink with a commercial desktop inkjet printer for wearable application at sub-GHz. A non-resonant coplanar monopole antenna has been closely placed on a miniaturized AMC to limit the radiating structure of area $0.14\lambda_0 \times 0.14\lambda_0$ at 700 MHz. Although there are various techniques of antenna designing and fabrication, techniques like printed antenna [24], triple mode antenna [25], triangular patch antenna [26], CPW-fed slot antenna [27], PIFA with dual resonance mode [28], screen-printed wearable and washable antennas [29], a butterfly-shaped microstrip patch antenna [30] have gained attention in the design of wideband wearable antenna for healthcare applications.

In perspective of these, wearable antennas are very popular due to their easy availability and easy fabrication with our day-to-day clothes. Also, it can be easily embedded into clothing materials. Earlier antennas were used to fabricate with substrate material like FR4, RT duroid, etc, where it was difficult to obtain the flexible nature of the antenna and also its characteristics. Presently, flexible wearable antennas with a variety of different substrates like denim, felt, Velcro, foam, PDMS, and different shapes are widely available.

In this paper, a foam-based compact flexible wideband antenna for healthcare application is realized using copper foil as a radiating patch and foam as the dielectric material. This compact structure can work in a wide range of frequencies from 2.9 to 9.94 GHz which makes it the right choice for wideband wearable antennas. This paper is organized as follows. Section 1 introduces wearable antennas and the literature on related work. Section 2 details the antenna structure. Section 3 compares simulated and measured results, and Sections 4 through 6 perform bending, on-body, and SAR analysis. Section 7 provides a discussion of the results obtained. In Section 8, a conclusion is drawn for the proposed antenna.

2. ANTENNA STRUCTURE

The intended structure of an antenna is derived from a rectangular patch geometry which is later shaped into a hexagonal geometry as shown in Figure 2. The width of the hexagon (W_h) is taken out as half of the patch width ($W_p/2$). The foam thickness of 2 mm is utilized as a flexible substrate. Its dielectric constant (ε_r) is taken as 1.07 and the loss tangent ($\tan\delta$) as 0.0025 [33–35]. The foam substrate is chosen due to low cost, wide availability, and its flexible nature to integrate with the wearer's clothes.

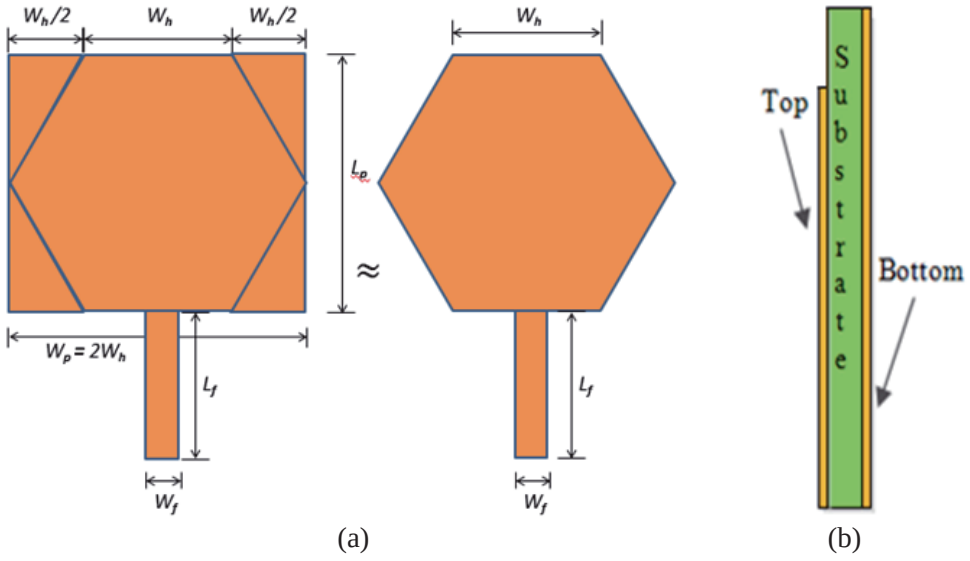

Figure 2. Geometry of Hexagonal Microstrip Patch Antenna (HMSA). (a) Rectangular to hexagonal geometry. (b) Side view.

The radiating patch and ground plane of an antenna are formed by using a 0.05 mm thick copper foil. The theoretically designed antenna is simulated in Ansys HFSS simulation software and optimized to get the desired result.

2.1. Design of Hexagonal Microstrip Patch Antenna (HMSA)

The proposed HMSA is designed with Equations (1) to (4) [31] to have a resonating structure of a compact microstrip antenna. Equation (1) describes the resonating frequency whereas Equations (2) to (4) are used to get an effective dielectric constant and the width of the patch.

2.1.1. Case I: Design with Full Ground

A theoretically designed geometry is simulated in Ansys HFSS simulation software with the full ground plane as per Table 1 parametric values. The geometry is shown in Figures 3(a) & (b).

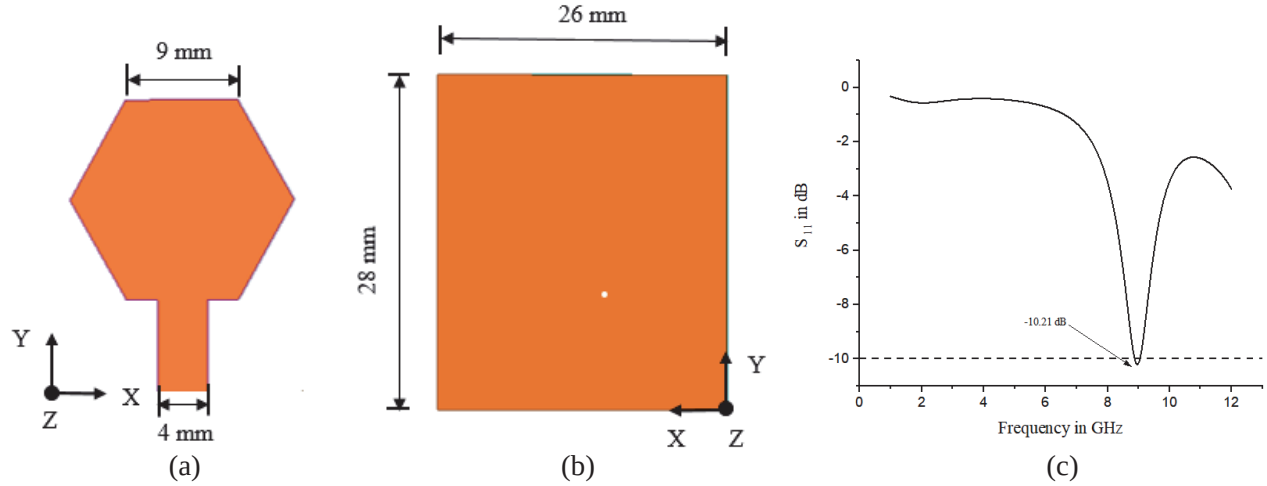

Figure 3. Geometry of Compact HMSA with full ground plane and its return loss. (a) Front view. (b) Back view. (c) Return loss with full ground plane.

Table 1. Design parameters of compact HMSA.

Parameter	W_h	h	t	L_{sub}	W_{sub}	L_g	W_g	L_f	W_f
Value (mm)	9	2	0.05	28	26	28	26	7.1	4

The result obtained with the full ground plane is shown in Figure 3(c). The antenna resonates nearly at 9.01 GHz with poor matching which results in a narrow bandwidth of 0.250 GHz.

2.1.2. Case II: Design with Partial Ground

Considering the poor return loss and bandwidth (0.25 GHz) obtained with the full ground, the performance of the wearable wideband antenna cannot be satisfactory. The same patch structure is used with the reduction in the size of the ground to improve the performance of the antenna. The length of the ground plane is reduced drastically as $L_g = 7$ mm; however, the width is kept the same as the earlier design to consider it as a partial ground rather than full. The modelled geometry is shown in Figures 4(a) & (b).

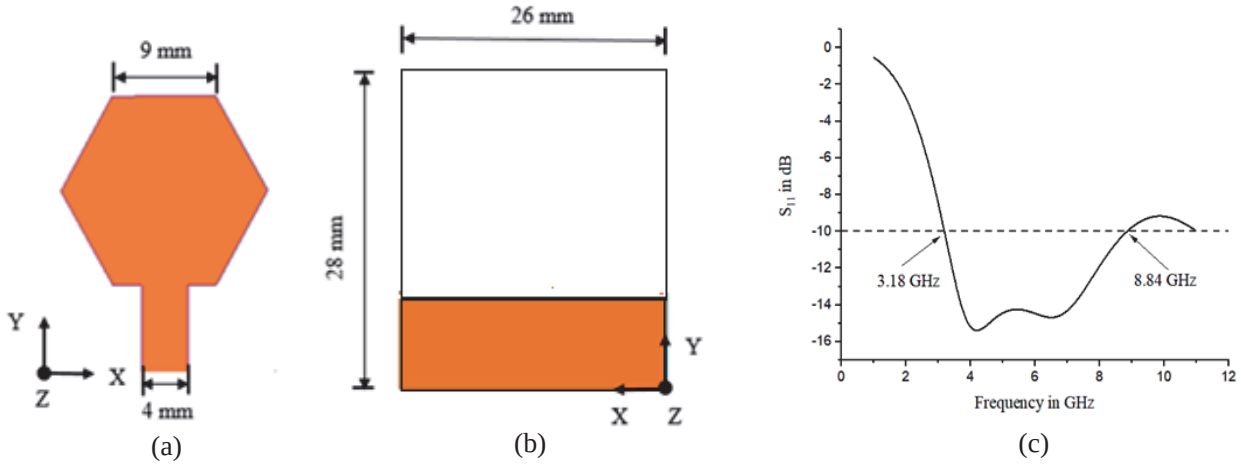

Figure 4. Geometry of compact HMSA with the partial ground. (a) Front view. (b) Back view. (c) Return loss characteristics.

With the reduction in the width of the ground plane, the performance of the compact HMSA is improved considerably. The value of the performance parameter is swapped as presented in Figure 4(c). With the partial ground technique, a wideband operation is achieved from 3.18 to 8.84 GHz. This simple HMSA with partial ground gives a maximum value of return loss of -15.34 dB and a bandwidth of 5.6284 GHz which is better than the the full ground. Observing Figure 4(c), the matching in terms of returns loss and bandwidth can also be improved with the cutting of a slot into the present geometry.

2.1.3. Case III: Slot Cut Design

In this design, the slot is created at the bottom left side of the hexagon to observe an enhancement in the return loss characteristic and bandwidth. Considering the slot dimension as $l_1 = 3.05$ mm and $w_1 = 5.87$ mm, the geometry is designed and shown in Figure 5(a). The slot dimensions are optimized in terms of length to have a resonating structure below -10 dB.

The simulated results obtained by cutting a slot are presented in Figure 5(b). The foremost thing with this structure is an enhancement in the bandwidth, and the tuning of the antenna is also good at the frequencies 3.7 GHz and 7 GHz with the maximum value of S_{11} as -28.29 dB.

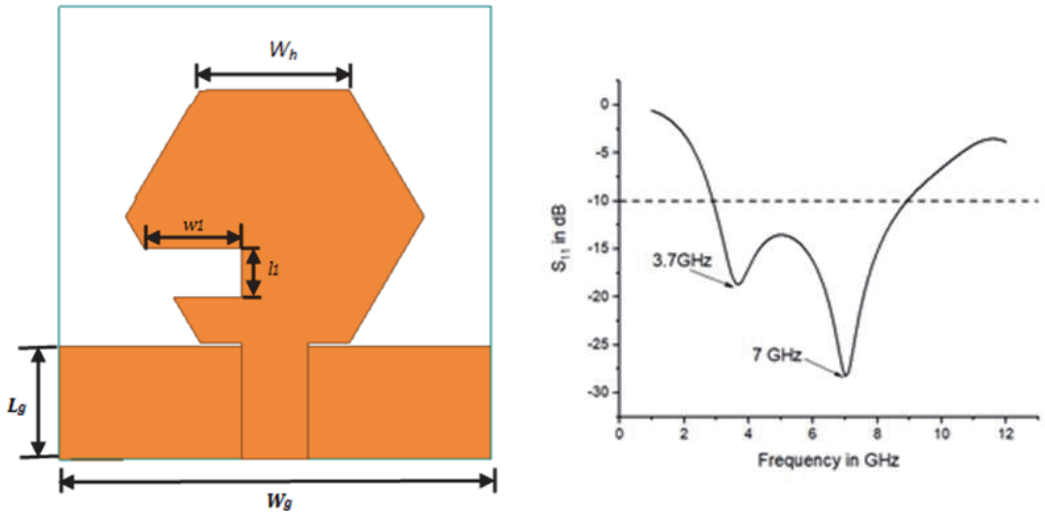

Figure 5. Geometry of compact HMSA with a slot. (a) Front and back view. (b) Return loss characteristic.

2.1.4. Case IV: Two Slots Cut Design

The simulated results obtained in the geometry with a single slot are satisfactory in getting the operation over a wideband structure. With the same dimension of length and width as the first slot, a second slot is created at the top left side of the hexagon to observe the behaviour of the antenna. The design parameters are depicted in Table 2, and the geometry is shown in Figure 6(a).

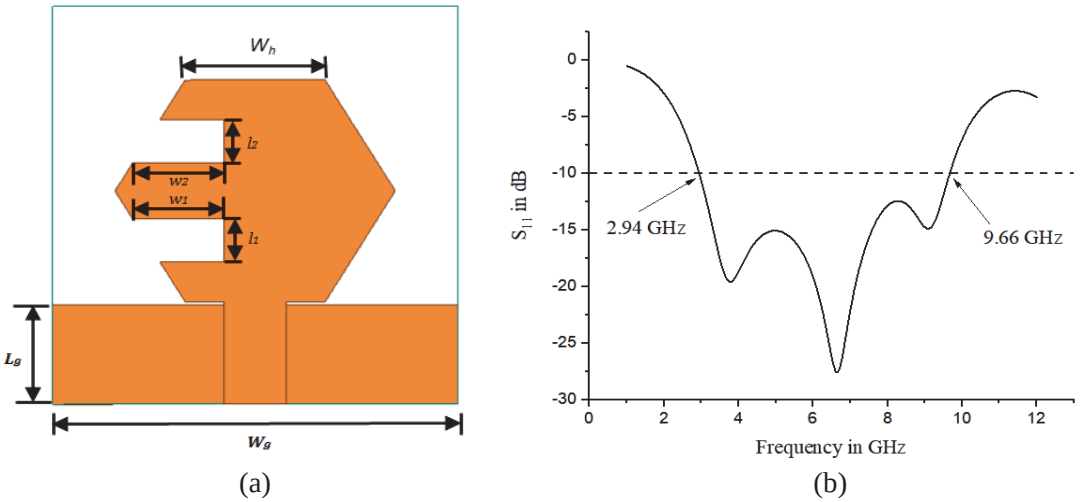

Figure 6. Geometry of compact HMSA with two slot. (a) Front and back view. (b) Return loss characteristic.

Table 2. Design parameters for two slot geometry.

Parameter	W_h	h	t	L_{sub}	W_{sub}	L_g	W_g	L_f	W_f	$l_1 = l_2$	$w_1 = w_2$
Value (mm)	9	2	0.05	28	26	7	26	7.1	4	3.05	5.87

The results obtained with the two slots are quite promising in the case of bandwidth and return loss parameters. The designed structure resonates at three different frequencies: 3.8 GHz, 6.7 GHz, and 9.1 GHz. The parametric improvement is seen good with two slots in compact HMSA and presented in Figure 6(b). The stage-wise evolution of all the structures is shown in Figure 7 whereas the performance comparison of all stages in terms of return loss characteristics is marked in Figure 8 and presented in Table 3.

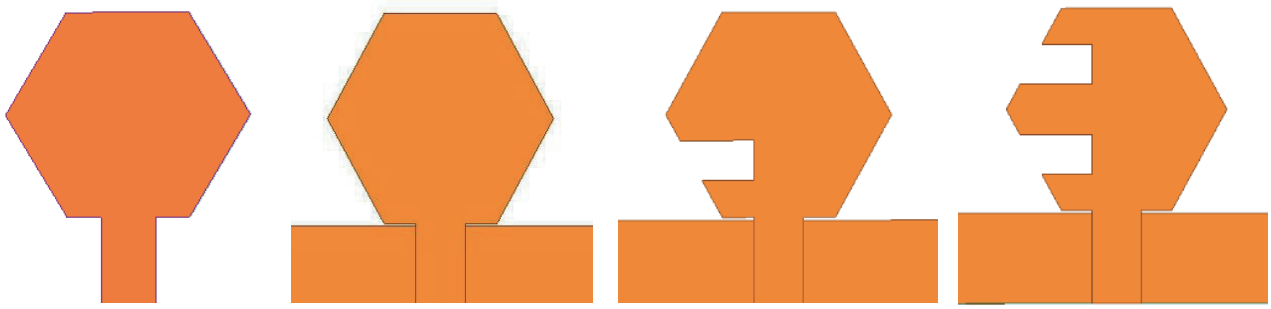

Figure 7. Geometry variation of compact HMSA. (a) Full ground. (b) Partial ground. (c) With a slot. (d) With two slot.

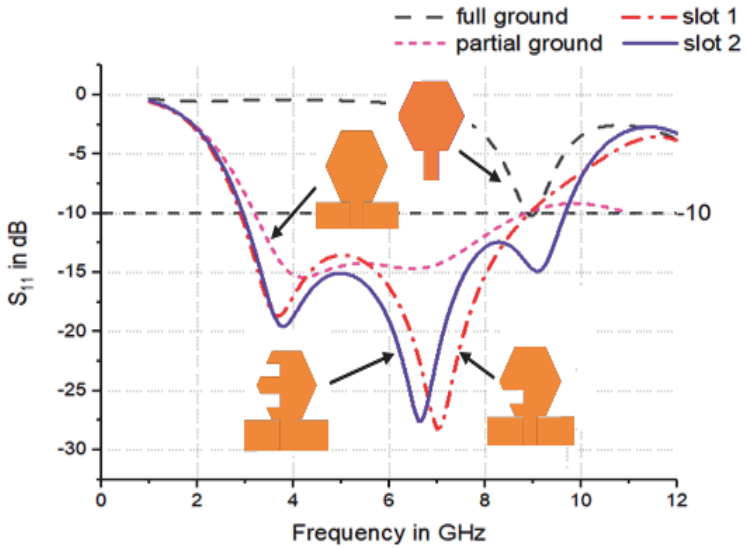

Figure 8. Return loss performance with variation in geometry.

Table 3. Parametric results with geometry variation.

Parameter/geometry	full ground	partial ground	With a slot	With two slot
Resonating frequency (GHz)	9.01	4.2, 6.6	3.7, 7	3.8, 6.7, 9.1
Bandwidth (GHz)	0.250	5.62	6.01	6.71

3. SIMULATED AND MEASURED RESULTS

The simulated results obtained with two slots are promising and intended for prototype fabrication. Considering the dimensions of Table 2 along with copper foil as a radiating patch as well as partial ground plane element and flexible foam as a dielectric substrate, the prototype of two slot compact HMSA is created. Photographs of the fabricated prototype are shown in Figure 9.

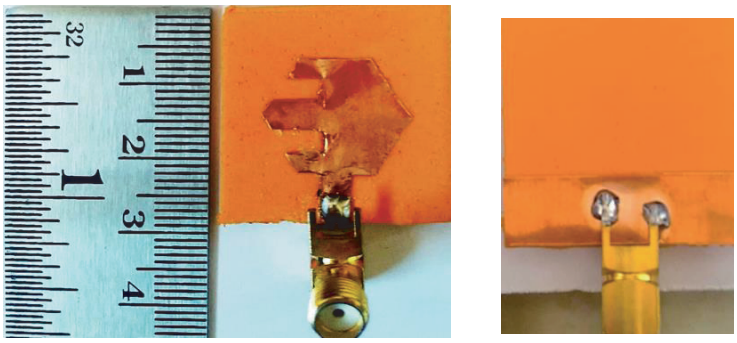

(a) (b)

Figure 9. Photograph of fabricated compact flexible HMSA. (a) Front view. (b) Back view.

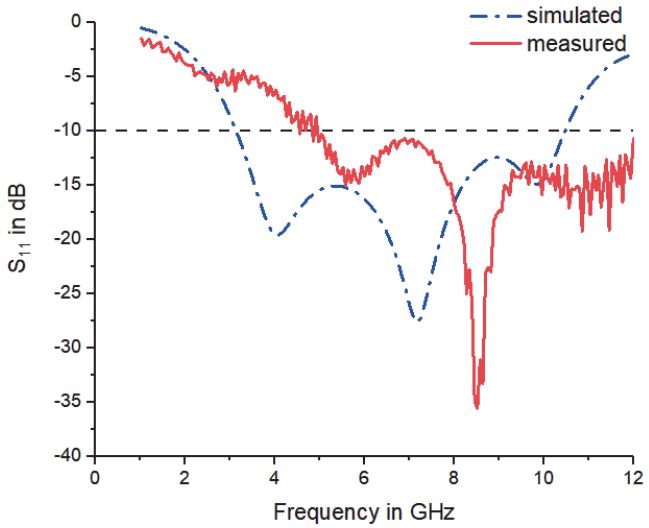

Figure 10. Comparison of simulated and measured S_{11}.

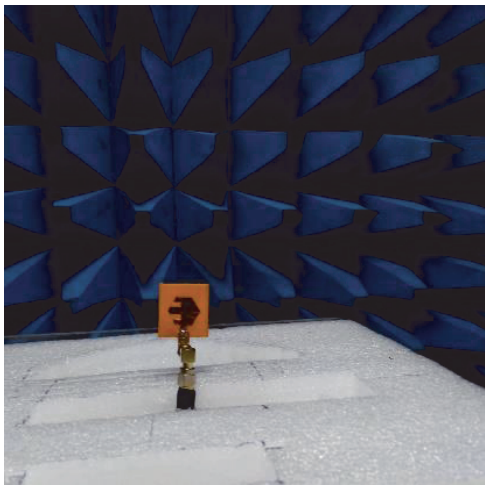

Figure 11. Photograph of radiation pattern measurement setup inside an anechoic chamber.

The results obtained are slightly shifted and can be seen in Figure 10. The shifting may arises due to the manual fabrication of the antenna. The discrepancies between the measured and simulated results are attributed to small fabrication errors and assembly inexactness. The antenna radiation pattern is also measured with the setup of an anechoic chamber as shown in Figure 11. The simulated values of radiation done by the antenna in the E-plane and H-plane are shown in Figure 12, whereas Figure 13 shows the measured radiation pattern for the same plane. The measured radiation patterns are obtained in an anechoic chamber using an Antenna Measurement System in combination with a Rohde and Schwarz ZVL Network Analyser of frequency range 10 K to 40 GHz. Referring to the coordinate system in which the antenna is placed (Figure 3), the E-plane is taken to be the XZ plane (or phi = 0 degrees) while the H-plane is taken to be the YZ-plane (or phi = 90 degrees). A good agreement was found between the simulated and measured radiation patterns at several points of

radiation w.r.t. three different frequencies. The maximum gain is observed at a frequency of 9.1 GHz whereas at some frequencies, a shift in radiation pattern is observed.

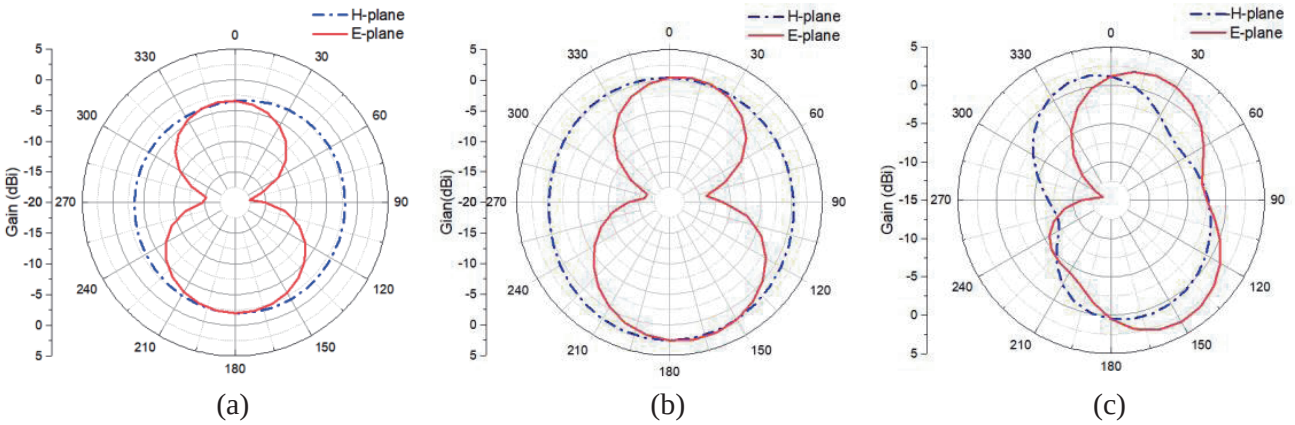

Figure 12. Simulated radiation pattern in E-plane and H-plane. (a) 3.8 GHz. (b) 6.7 GHz. (c) 9.1 GHz.

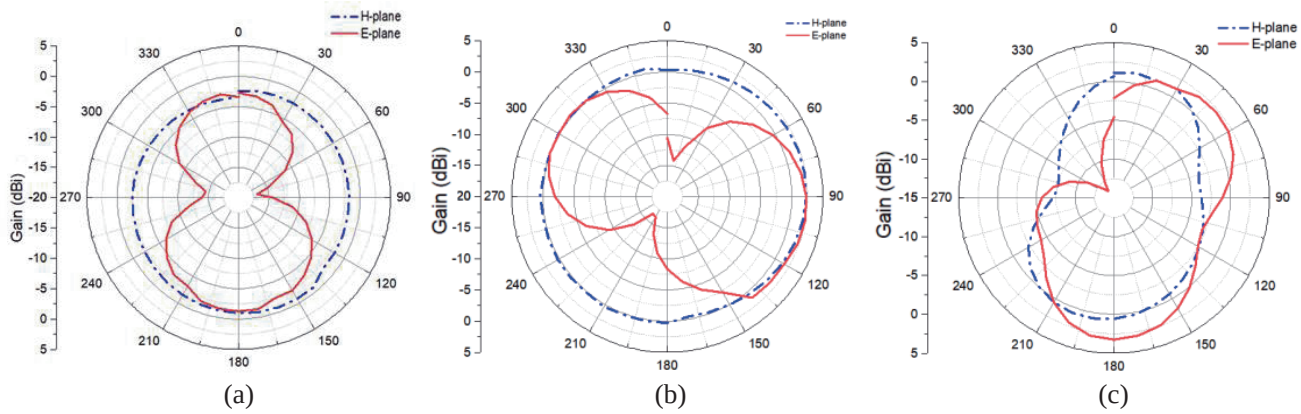

Figure 13. Measured radiation pattern in E-plane and H-plane. (a) 3.8 GHz. (b) 6.7 GHz. (c) 9.1 GHz.

The current distribution at three different frequencies is presented in Figure 14. At all the frequencies, almost a very good impedance matching is observed.

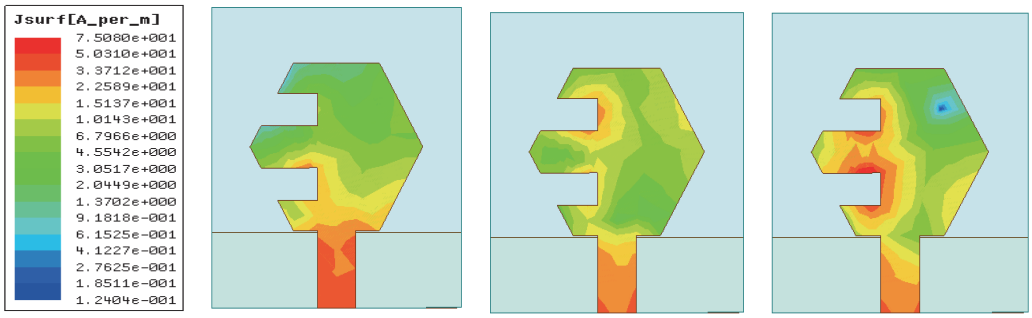

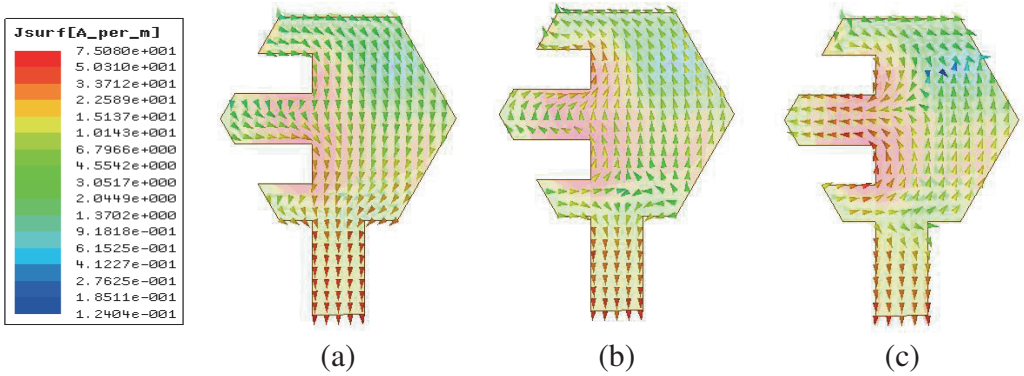

Figure 14. Current distribution at different resonating frequencies. (a) 3.8 GHz. (b) 6.7 GHz. (c) 9.1 GHz.

4. BENDING ANALYSIS

The wearable antennas may be detuned when it is folded or bent. To consider the performance of the flexible antenna, conformal analysis is carried out in HFSS. As depicted in Figures 15(a) and (b), the antenna is enfolded around a hollow cylindrical pipe with radii of 24 mm and 11 mm. Figure 15(c) represents the fluctuation of S_{11} under bent conditions. One can see that the frequency change makes the proposed antenna almost resistant to bending. Though the frequency is shifted slightly, it can be neglected considering the performance under folding conditions.

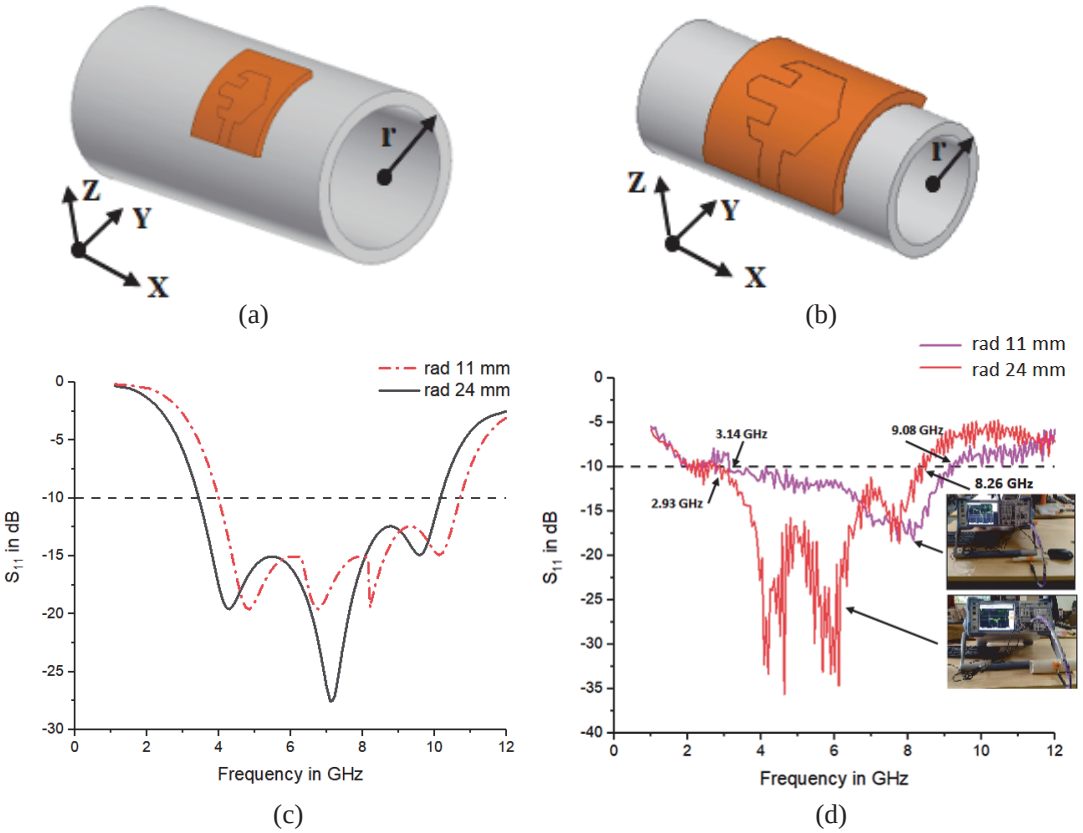

Figure 15. Bending performance of the proposed antenna at radius 24 mm and 11 mm. (a) Bending with radius $r = 24$ mm. (b) Bending with radius $r = 11$ mm. (c) Comparison of simulated S_{11}. (d) Comparison of measured S_{11}.

As seen in Figure 15(d), two PVC pipes with radii of 24 mm and 11 mm are used to analyse the bending performance of an antenna physically. To prevent movement while doing the measurement, the antenna is wrapped around the pipe and cinched down with the aid of plastic sticky tape. Under two different radii of pipe, a Vector Network Analyzer is utilised to assess return loss. The results are good for impedance match below −10 dB. It has been observed that with a bending radius of 24 mm, the maximum value of S_{11} is marked as −35.60 dB along with the bandwidth of 5.33 GHz. However, the antenna's bandwidth performance (5.94 GHz) is improved at a bending radius of 11 mm. The proposed antenna performs very well under different bending circumstances.

5. ON-BODY ANALYSIS

At higher frequencies, human tissues have a lossy nature. Antenna parameters are significantly impacted such as resonance frequency, bandwidth, and radiation pattern by the electromagnetic properties of tissues. Antenna performance suffers when a person is nearby. Figure 16(a) illustrates the creation of a tissue equivalent body phantom model using the three layers of skin, fat, and muscle with HFSS. This phantom model is 50 mm × 50 mm × 27 mm in size and 2 mm, 5 mm, and 20 mm thick, respectively. The electrical characteristics of skin, fat, and muscle layers are determined [40, 41] over the frequency range of 2.9 to 9.6 GHz. The relative permittivity, conductivity, loss tangent, and mass density values depicted in Table 4 are taken into account for the simulation of SAR at the frequency of 3.8, 6.7, and 9.1 GHz. The return loss characteristic S_{11}, VSWR (< 2), and front to back ratio simulated over phantom model are presented in Figures 16(b), (c), and (d). The radiation patterns at 3.8, 6.7, and 9.1 GHz are also

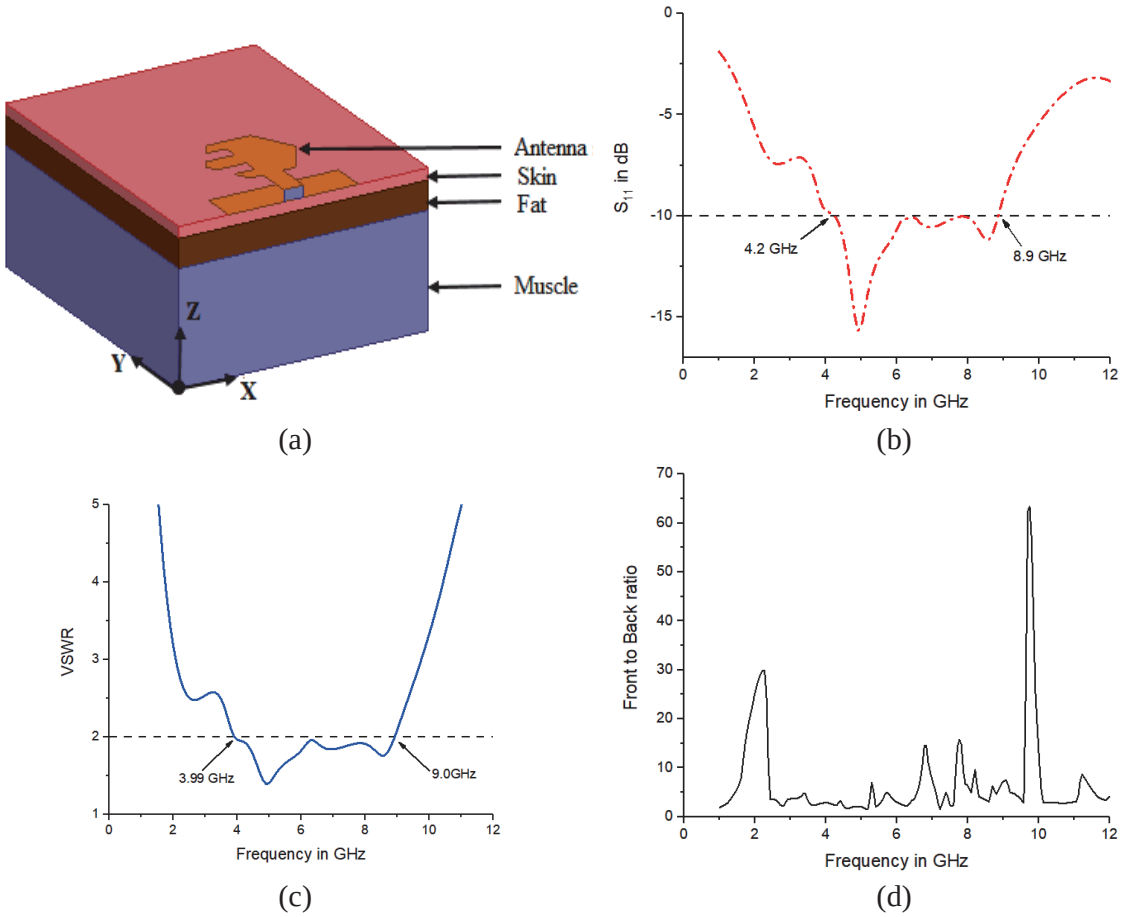

Figure 16. Simulated results on a three-layer tissue equivalent body phantom model. (a) Three-layer tissue equivalent body phantom model. (b) Return loss (S_{11}) characteristics. (c) VSWR. (d) Front-to-back ratio.

Table 4. Electrical characteristics of skin, fat and muscle tissue.

Tissue	Frequency (GHz)	Conductivity σ (S/m)	Permittivity (ε_r)	Loss tangent	Mass density (kg/m^3)
Skin (dry)	3.8	2.2105	36.753	0.28451	1109
	6.7	4.5305	34.346	0.35389	
	9.1	7.0049	32.155	0.43032	
Fat	3.8	0.17175	5.1444	0.15792	911
	6.7	0.35307	4.874	0.19435	
	9.1	0.52093	4.6724	0.22023	
Muscle	3.8	2.8275	51.072	0.26189	1090
	6.7	6.0738	47.273	0.34471	
	9.1	9.3341	43.989	0.41915	

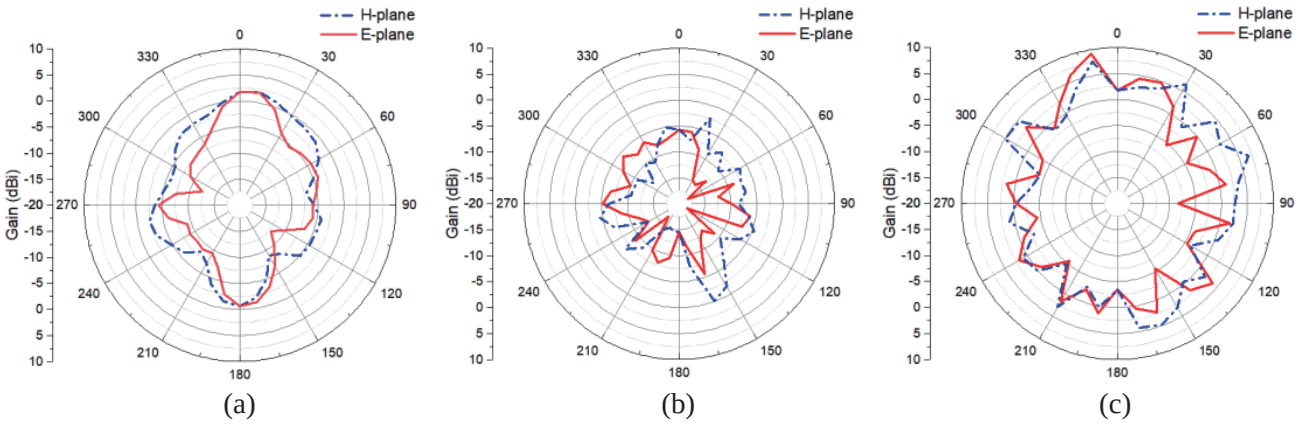

Figure 17. Radiation pattern simulated on a three-layer tissue equivalent body phantom model. (a) 3.8 GHz. (b) 6.7 GHz. (c) 9.1 GHz.

simulated over phantom model and shown in Figure 17.

The actual measurement in the presence of human body for return loss is performed on the skin and cloth. The antenna is placed on the arm and chest of the human body of 80 kg in weight and 178 cm in height as shown in Figures 18(a) and (b).

The results obtained by testing over the skin and chest of the human body give a good impedance matching below −10 dB. It has been observed from Figure 18(c) that the proposed antenna exhibits a satisfactory bandwidth of 5.1 GHz under both conditions of testing.

6. SAR ANALYSIS

Specific Absorption Rate (SAR) values depend on the dielectric constant of tissues. The SAR value is calculated on 10 grams of tissue for the designed three-layer tissue phantom model. For the 10 grams of tissue, the RF safety limit is 2 W/kg as per European standards [32, 42]. The average 10 gm SAR of antenna has been studied on a flat phantom model designed with a size of 50 mm × 50 mm × 27 mm. Input power of 1 mW is applied in HFSS to evaluate the SAR values at three different frequencies as 3.8, 6.7, and 9.1 GHz. The maximum average SAR values are 0.585 W/kg, 1.88 W/kg, and 1.9 W/kg w.r.t. frequencies stated. The SAR values obtained on the phantom model at respective frequencies are depicted in Figure 19. The obtained SAR values are within the IEEE standards threshold of safety limit of less than 2 W/kg.

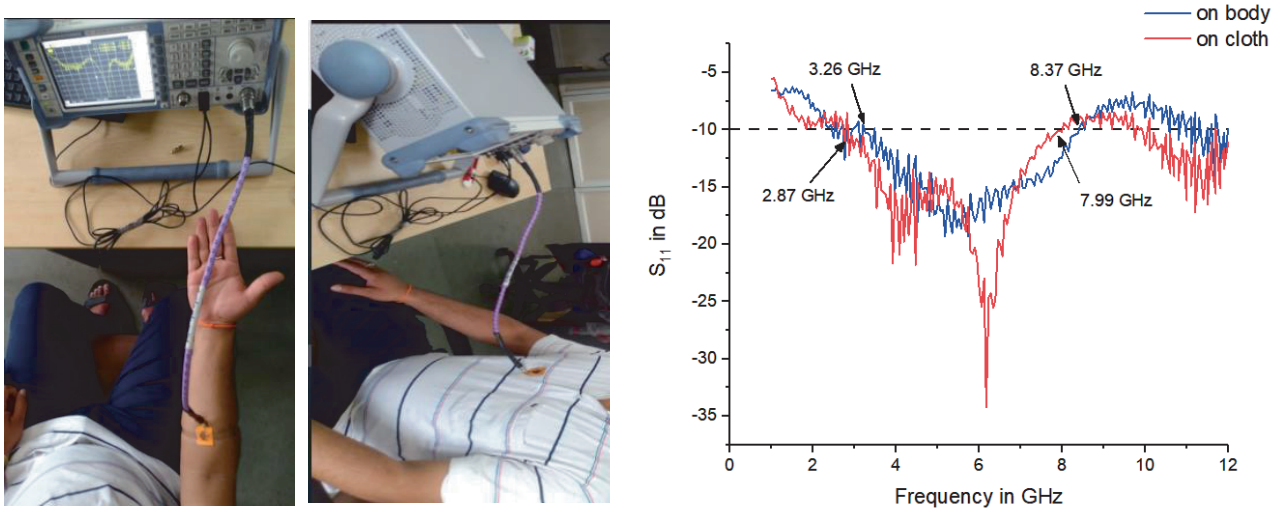

(a) (b) (c)

Figure 18. On-body performance of antenna. (a)–(b) Photograph of antenna placement on arm and chest. (c) Comparison of measured return loss (S_{11}) for arm and chest.

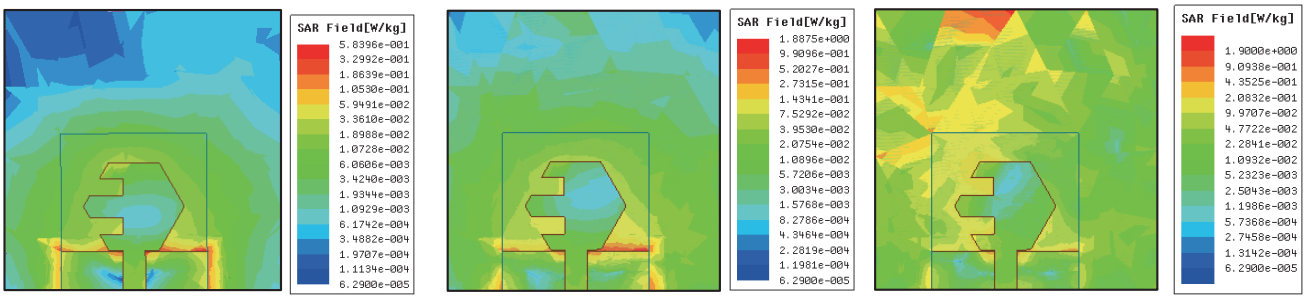

(a) (b) (c)

Figure 19. SAR analysis over 10 gm of tissue for the three-layer phantom model. (a) 3.8 GHz. (b) 6.7 GHz. (c) 9.1 GHz.

7. RESULTS AND DISCUSSIONS

The proposed antenna gives a good impedance matching below −10 dB for the reflection coefficient value. The antenna resonates at three different frequencies: 3.8, 6.7 and 9.1 GHz. The bandwidth expands from the lower frequency of 2.94 GHz to the upper frequency of 9.66 GHz resulting in a bandwidth of 6.71 GHz which gives an impedance bandwidth of 106.67%. The simulated and measured S_{11} characteristic of the fabricated two-slot compact HMSA is presented in Figure 10. The measured and simulated results are in good agreement with a slight shift in resonant frequency. The results obtained are compared with some previous work as presented in Table 5. It is clear that the proposed antenna is very compact as the side length is 9 mm. The antenna is mainly designed to operate at a high frequency; however, it works very well also at lower frequencies such as 3.8 and 6.7 GHz. The proposed antenna is validated for conformal nature by performing bending analysis at two different radii of 24 mm and 11 mm. Under bending state, the antenna resonates very well below −10 dB and produces a bandwidth of 5.33 GHz & 5.94 GHz, respectively. The on-body and SAR analysis is also performed over a 10 gm tissue resulting in a maximum SAR value of 1.9 W/kg within the safety limit of less than 2 W/kg. The proposed antenna has a wide range of frequencies from 2.94 to 9.66 GHz which is helpful for many healthcare applications in the ISM band. The size of the antenna is very small and compact in shape; the antenna is well suited for wearable applications for the reason of the conformal nature of the dielectric material.

Table 5. Comparison of the proposed antenna with the previous work.

Ref.	Overall antenna dimension	Operating Frequency /Bandwidth	Substrate /dielectric constant (ε_r)	Conducting material	Gain
[36]	$60 \times 75 \times 0.125\,\text{mm}^3$	7–13 GHz /60.00%	PET (3.2)	Conductive Silver ink	5 dBi
[37]	$0.44 \times 0.4 \times 0.002\lambda_g^3$	3.3–3.88 GHz /17.57%	Kapton Polyimide (3.5)	Copper	2.06 dBi
[38]	$60 \times 48 \times 0.8\,\text{mm}^3$ $(0.72 \times 0.57 \times 0.009\lambda_g^3)$	0.9–6 GHz /85%	Jeans (1.9)	Copper foil	2.6 dBi
[39]	$32 \times 42 \times 3\,\text{mm}^3$ $(0.38 \times 0.5 \times 0.036\lambda_g^3)$	3.14–5.45 GHz /31.84%	Felt (1.3)	ShieldIt conductive fabric	6 dBi
This work	$28 \times 26 \times 2\,\text{mm}^3$ $(0.78 \times 0.73 \times 0.056\lambda_g^3)$	2.94–9.66 GHz /106.67%	Foam (1.07)	Copper foil	4.67 dBi

8. CONCLUSION

This paper presents a compact flexible hexagonal shape microstrip patch antenna with foam as the substrate material. The light weight, low-cost manufacturing, and flexibility to fit conformal surfaces make the flexible antenna ideal for current and future wireless communication and sensing applications. The designed antenna resonates at three different frequencies, i.e., 3.8, 6.7, and 9.1 GHz over a wide range of frequencies ranging from 2.94 to 9.66 GHz. The measured and simulated results are found in good agreement, and the gain of 4.67 dBi is reported. The greatest advantage of using foam as a substrate is its dielectric constant (1.07), which has facilitated enhancement in the bandwidth and gain of the flexible antenna. Furthermore, the enhancement in the bandwidth of 106.67% is achieved with various iterations like converting a full ground to partial ground and thereby creating a slot. The proposed antenna has performed well under different bending conditions proving the conformal nature, and SAR analysis shows the use of the antenna for wearable healthcare applications as the right candidate by limiting the value of SAR below the safety limit of less than 2 W/kg for 10 gm of tissue.

ACKNOWLEDGMENT

The authors would like to acknowledge the Department of Electronics and Communication of R. V. College of Engineering, Bengaluru, India for providing a testing facility at the Centre of Excellence in Smart Antenna Systems and Measurements (SASM).

REFERENCES

1. Agiwal, M., A. Roy, and N. Saxena, "Next generation 5G wireless networks: A comprehensive survey," *IEEE Communications Surveys & Tutorials*, Vol. 18, No. 3, 1617–1655, 2016.
2. Karad, K. V. and V. S. Hendre, "Review of antenna array for 5G technology using mmwave massive MIMO," *Recent Trends in Electronics and Communication, Lecture Notes in Electrical Engineering*, Vol. 777, Springer, Singapore, 2020.
3. Keysight Technologies, "Keysight Technologies: The internet of things enabling technologies and solutions for design and test," *Application Notes*, 2016.
4. Ali, S. M., C. Sovuthy, M. A. Imran, S. Socheatra, Q. H. Abbasi, and Z. Z. Abidin, "Recent advances of wearable antennas in materials, fabrication methods, designs, and their applications: State-of-the-Art," *Micromachines*, Vol. 11, No. 10, 888, 2020.

5. CISCO, "CISCO Visual Networking Index: Global Mobile Data Traffic Forecast Update, 2014–2019," 1–48, 2015.
6. Paracha, K. N., S. K. A. Rahim, P. J. Soh, and M. Khalily, "Wearable antennas: A review of materials, structures, and innovative features for autonomous communication and sensing," *IEEE Access*, Vol. 7, 56694–56712, 2019.
7. Priya, A., A. Kumar, and B. Chauhan, "A review of textile and cloth fabric wearable antennas," *Int. J. Comput. Appl.*, Vol. 116, 1–5, 2015.
8. Soh, P. J., G.A.E. VandenBosch, M. Mercuri, and D. M.-P. Schreurs, "Wearable wireless health monitoring: Current developments, challenges, and future trends," *IEEE Microw. Mag.*, Vol. 16, 55–70, 2015.
9. Mahmood, S. N., A. J. Ishak, T. Saeidi, H. Alsariera, S. Alani, A. Ismail, and A. C. Soh, "Recent advances in wearable antenna technologies: A review," *Progress In Electromagnetics Research B*, Vol. 89, 1–27, 2020.
10. Badhan, K., "Analysis of different performance parameters of body wearable antenna — A review," *Advances in Wireless and Mobile Communications*, Vol. 10, No. 5, 735–745, 2017, ISSN 0973-6972.
11. Sun, H., Z. Zhang, R. Q. Hu, and Y. Qian, "Wearable communications in 5G: Challenge and enabling technologies," *IEEE Veh. Technol. Mag.*, Vol. 13, 100–109, 2018.
12. Ashraf, J., A. Jabbar, A. Arif, K. Riaz, M. Zubair, and M. Q. Mehmood, "A textile based wideband wearable antenna," *International Bhurban Conference on Applied Sciences and Technologies (IBCAST) 2021*, 938–941, 2021.
13. Ouyang, Y. and W. J. Chappell, "High-frequency properties of electro-textiles for wearable antenna applications," *IEEE Trans. Antennas Propag.*, Vol. 56, 381–389, 2008.
14. Zhao, B., J. Mao, J. Zhao, H. Yang, and Y. Lian, "The role and challenges of body channel communication in wearable flexible electronics," *IEEE Transactions on Biomedical Circuits and Systems*, Vol. 14, No. 2, 283–296, 2020.
15. El Atrash, M., M. A. Abdalla, and H. M. Elhennawy, "A wearable dual-band low profile high gain low SAR antenna AMC-backed for WBAN applications," *IEEE Transactions on Antennas and Propagation*, Vol. 67, No. 10, 6378–6388, 2019.
16. Kuang, Y., L. Yao, W. Zhang, D. Zhou, H. Luan, and Y. Qiu, "A novel textile dual-polarized antenna potentially used in body-centric system," *2016 IEEE International Conference on RFID Technology and Applications (RFID-TA)*, 77–80, 2016.
17. Simorangkir, R. B. V. B., Y. Yang, L. Matekovits, and K. P. Esselle, "Dual-band dual-mode textile antenna on PDMS substrate for body-centric communications," *IEEE Antennas and Wireless Propagation Letters*, Vol. 16, 677–680, 2017.
18. Iqbal, A., A. Smida, A. J. Alazemi, M. I. Waly, N. K. Mallat, and S. Kim, "Wideband circularly polarized MIMO antenna for high data wearable biotelemetric devices," *IEEE Access*, Vol. 8, 17935–17944, 2020.
19. Smida, A., A. Iqbal, A. J. Alazemi, M. I. Waly, R. Ghayoula, and S. Kim, "Wideband wearable antenna for biomedical telemetry applications," *IEEE Access*, Vol. 8, 15687–15694, 2020.
20. Arif, A., M. Zubair, M. Ali, M. U. Khan, and M. Q. Mehmood, "A compact, low-profile fractal antenna for wearable on-body WBAN applications," *IEEE Antennas and Wireless Propagation Letters*, Vol. 18, No. 5, 981–985, 2019.
21. Yan, S., P. J. Soh, and G. A. E. Vandenbosch, "Wearable dual-band magneto-electric dipole antenna for WBAN/WLAN applications," *IEEE Transactions on Antennas and Propagation*, Vol. 63, No. 9, 4165–4169, Sept. 2015.
22. Mohd Rais, N. H., P. J. Soh, M. F. A. Malek, and G. A. E. Vandenbosch, "Dual-band suspended-plate wearable textile antenna," *IEEE Antennas and Wireless Propagation Letters*, Vol. 12, 583–586, 2013.
23. Genovesi, S., F. Costa, F. Fanciulli, and A. Monorchio, "Wearable inkjet-printed wideband antenna by using miniaturized AMC for sub-GHz applications," *IEEE Antennas and Wireless Propagation Letters*, Vol. 15, 1927–1930, 2016.

24. Sabban, A., "New wideband printed antennas for medical applications," *IEEE Transactions on Antennas and Propagation*, Vol. 61, No. 1, 84–91, Jan. 2013.
25. Zhang, K., Z. H. Jiang, W. Hong, and D. H. Werner, "A low-profile and wideband triple-mode antenna for wireless body area network concurrent on-/off-body communications," *IEEE Transactions on Antennas and Propagation*, Vol. 68, No. 3, 1982–1994, Mar. 2020.
26. Bhattachaijee, S., S. Teja, S. R. B. Chaudhuri, and M. Mitra, "Wearable triangular patch antenna for ON/OFF body communication," *2017 IEEE Applied Electromagnetics Conference (AEMC)*, 1–2, 2017.
27. Shanmuganantham, T., K. Balamanikandan, and S. Raghavan, "CPW-fed slot antenna for wideband applications," *International Journal of Antennas and Propagation*, Vol. 2008, Article ID 379247, 4 pages, 2008.
28. Gao, G., C. Yang, B. Hu, R. Zhang, and S. Wang, "A wide-bandwidth wearable all-textile PIFA with dual resonance modes for 5 GHz WLAN applications," *IEEE Transactions on Antennas and Propagation*, Vol. 67, No. 6, 4206–4211, Jun. 2019.
29. Scarpello, M. L., I. Kazani, C. Hertleer, H. Rogier, and D. Vande Ginste, "Stability and efficiency of screen-printed wearable and washable antennas," *IEEE Antennas and Wireless Propagation Letters*, Vol. 11, 838–841, 2012.
30. Sun, L., M. He, J. Hu, Y. Zhu, and H. Chen, "A butterfly-shaped wideband microstrip patch antenna for wireless communication," *International Journal of Antennas and Propagation*, Vol. 2015, Article ID 328208, 8 pages, 2015.
31. Ray, K. P. and M. D. Pandey, "Resonance frequency of hexagonal and half hexagonal Microstrip antennas," *Microwave and Optical Technology Letters*, Vol. 51, No. 2, 448–452, 2009.
32. Atanasova, G. and N. Atanasov, "Small antennas for wearable sensor networks: Impact of the electromagnetic properties of the textiles on antenna performance," *Sensors*, Vol. 20, No. 18, 5157, 2020.
33. Hatte, J. and V. Hendre, "Dwindle coupled loop antenna system for 5G communication applications," *J. Commun. Technol. Electron.*, Vol. 66, S100–S108, 2021.
34. Joshi, M. P., J. G. Joshi, and S. S. Pattnaik, "Hexagonal slotted wearable microstrip patch antenna for body area network," *2019 IEEE Pune Section International Conference (PuneCon)*, 1–4, 2019.
35. Joshi, J. G., S. S. Pattnaik, and S. Devi, "Metamaterial embedded wearable rectangular microstrip patch antenna," *International Journal of Antennas and Propagation*, Vol. 2012, Article ID 974315, 9 pages, 2012.
36. Tighezza, M., S. K. A. Rahim, and M. T. Islam, "Flexible wideband antenna for 5G applications," *Microwave and Optical Technology Letters*, Vol. 60, No. 1, 38–44, 2017.
37. Kumar Naik, K. and D. Gopi, "Flexible CPW-fed split-triangular shaped patch antenna for WiMAX applications," *Progress In Electromagnetics Research M*, Vol. 70, 157–166, 2018.
38. Khajeh-Khalili, F. and Y. Khosravi, "A novel wearable wideband antenna for application in wireless medical communication systems with jeans substrate," *The Journal of The Textile Institute*, 1–7, 2020.
39. Elias, B. Q. and P. J. Soh, "Design of a wideband spring textile antenna for wearable 5G and IoT applications using characteristic mode analysis," *Progress In Electromagnetics Research M*, Vol. 112, 177–189, 2022.
40. Hasgall, P. A., F. Di Gennaro, C. Baumgartner, E. Neufeld, B. Lloyd, M. C. Gosselin, D. Payne, A. Klingenböck, and N. Kuster, "IT'IS Database for thermal and electromagnetic parameters of biological tissues," Version 4.1, Feb. 22, 2022.
41. http://niremf.ifac.cnr.it/tissprop/htmlclie/htmlclie.php.
42. Doddipalli, S., A. Kothari, and P. Peshwe, "A low profile ultrawide band monopole antenna for wearable applications," *International Journal of Antennas and Propagation*, Vol. 2017, Article ID 7362431, 9 pages, 2017.